

## Chapter 4 - Silicate glasses and glass-ceramics: types, role of composition and processing methods

Dilshat Tulyaganov <sup>1,\*</sup>, Francesco Baino <sup>2</sup>

<sup>1</sup> Department of Natural-Mathematical Sciences, Turin Polytechnic University in Tashkent, Tashkent, Uzbekistan

<sup>2</sup> Institute of Materials Physics and Engineering, Department of Applied Science and Technology, Politecnico di Torino, Turin, Italy

\* tulyaganovdilshat@gmail.com

**Abstract.** Glass has been a versatile and fascinating material since the early stages of civilization. The aesthetic and functional properties of glasses are mainly dictated by the composition, which in most cases is a mixture of inorganic oxides and can be properly designed according to the end use. Glass-ceramics are polycrystalline materials produced by the controlled crystallization of certain parent glasses and contain one or more crystalline phases embedded in a residual amorphous matrix. The distinct chemical nature and microstructural features of these phases have led to various combinations of properties and applications in many industrial, medical and high-tech fields. This chapter introduces the reader into the “mystery of glass”, providing a picture of the structural theories, formation criteria and main processing methods for glass and glass-ceramic products with focus on a selected set of silicate materials..

**Keywords:** Glass; Glass-Ceramic; Melt-quenching; Sol-gel; Crystallization; Sintering.

### 1 Definition of glass: the attempts to disclose its secret

Glass is indeed one of the most “universal” and fascinating materials made by mankind. Use and evolution of glass products have often been associated to key steps from technological, historical and societal viewpoints over the long path of human progress. Generally speaking, the term “glass” refers to a fragile and transparent matter having a dramatically broad range of current applications in arts, building, industry, medicine, optics and optoelectronics, and everyday life [1-14]. Although the most traditional glasses are inorganic and non-metallic, the term “glass” has been gradually extended to include optically-transparent high-quality polymers (the so-called organic glasses, e.g. poly(methyl methacrylate)) and amorphous metals (also called metallic glasses).

According to the ASTM definition of glass, as initially proposed by Committee C-14 in the tentative standard about glass in 1941 and still issued in ASTM C162 in 1992, glass is an inorganic product of melting which has been cooled to a rigid condition without undergoing crystallization [15,16]. This definition is valid for most

commercial glasses but does not take into account some “modern” alternative methods to produce glasses, such as vapor deposition, sol-gel process and neutron irradiation of crystalline materials.

From a general viewpoint, glass is typically hard and brittle, and exhibits a conchoidal fracture. It may be colourless or coloured, and its optical transparency to visible light can vary depending on the presence of crystalline phases embedded in the glassy matrix. These glass-crystal composites are actually called glass-ceramics; devitrification (i.e. the nucleation and growth of crystalline phases inside glass) make the material partially or totally opaque.

Many other definitions for glass have been proposed over the last decades, including the attempt to distinguish between glass and amorphous solids (not all amorphous solids can be considered as glasses: for example, wood and amorphous silicon are actually amorphous but exhibit no glass transition temperature) and the concept of supercooled liquid (however, glass does not exhibit any viscous flow at room temperature) [1,6,8,13]. Perhaps, the most fascinating definition of glass was provided by Prof. Patrick Charbonneau in a press release of Duke University in 2014: “glass is a mystery”. He also added: “There have been beautiful mathematical models, but with sometimes tenuous connection to real, structural glasses. Now we have a model that is much closer to real glasses”. In fact, Prof. Charbonneau used advanced mathematical theories to analyze how glass molecules behave and concluded that glasses seem to obey fractal models.

Finally, a practical definition of glass can be provided on a phenomenological basis: glasses have no long-range, periodic atomic arrangement, and exhibit a time-dependent glass transformation behaviour. This behaviour occurs over a temperature range known as the glass transformation region. Hence, any material (inorganic, organic, or metallic) formed by any technique, which exhibits glass transformation behaviour, is a glass [5].

Most common glasses are formed via rapid cooling of melts in order to avoid crystallization, since little time is allowed for the atomic ordering processes. The glass transformation behaviour is usually analysed and discussed by plotting the volume (or enthalpy) vs. temperature (Fig. 1) [5,14,17]. Most liquids upon cooling abruptly solidify at a fixed temperature,  $T_m$  (the melting point or liquidus temperature), with a significant change in volume following the line b-c in the diagram shown in Fig. 1. This is due to the formation of a long-range, periodic atomic arrangement. Continued cooling of the crystal will result in a further decrease in volume due to the heat capacity of the crystal. If the rate of *thermal* energy removal is *faster* than the rate of *crystallization*, the latter will not occur and the material can be considered as a supercooled liquid, while the volume follows the line b-e in Fig. 1. The viscosity of the supercooled melt continues to increase as the temperature is reduced until a temperature is reached, called glass transition temperature ( $T_g$ ), around which the volume-temperature plot undergoes a significant change in slope (“knee point”). Below  $T_g$ , the material can be considered rigid and solid for most practical applications [3,5]. This temperature range around  $T_g$ , the limits of which correspond to the enthalpies of equilibrium liquid and frozen solid, is known as the transition (or transformation) range; here, the viscosity of glass is about  $10^{12}$  Pa·s [3,5]. Glass transition corresponds to the transition from the liquid state to the glassy state (or the reverse one); in a disordered liquid, each structural unit can thermally diffuse over the whole size of the

system while, in the glassy state, such a thermal motion is restricted within a cage of nearest neighbors due to ultrahigh viscosity (internal attrition). However, only below  $T_g$  the material descended from the frozen melt may be correctly referred to as a glass [5,14]. At room temperature, the glass exhibits a structure similar to that which was frozen in the melt at  $T_g$ . Below  $T_g$  a glass, like supercooled liquid, has a higher free energy than a crystalline phase due to the fact that the energy absorbed during fusion of crystals was not completely given up during glassy solidification [7]. Hence, glasses are thermodynamically metastable solids and tend to spontaneously evolve towards the crystalline state (devitrification). However, since structural rearrangements can occur just extremely slowly at temperatures well below  $T_g$ , glasses can be considered stable for practical purposes.

The definition and understanding of the glassy state are fundamental to glass science and technology. A concise picture of the complexity of the glassy state, which combines features of both liquids and solids and also brings along its own peculiar characteristics, was effectively provided in 2017 by Zanotto and Mauro [17] as follows: (i) glass is non-crystalline and thus is absent of long-range atomic order which is characteristic of most solid materials; (ii) the structure of glass is very similar to that of its parent supercooled liquid; (iii) glass is a non-equilibrium solid, meaning that the glassy state cannot be described using equilibrium thermodynamics or statistical mechanics and the macroscopic properties of a glass depend on composition and thermal history; (iv) a glass is frozen by quenching from the liquid state, but over longer times it indeed flows and relaxes toward the supercooled liquid state; (v) glasses relax and then crystallize upon continuous heating at any temperature above absolute zero. As a result, an alternative definition for glass was then proposed: “Glass is a non-equilibrium, non-crystalline condensed state of matter that exhibits a glass transition. The structure of glasses is similar to that of their parent supercooled liquids (SCL), and they spontaneously relax toward the SCL state. Their ultimate fate is to solidify, i.e., crystallize” [17]. The last part of this definition was criticized by Schmelzer and Tropin [18] who suggested that “even if this statement would be true, it seems to us not to be reasonable to include such a statement into the definition, as it does not supply any additional information as to what glasses are. In addition, if at all, crystallization proceeds at a perceptible rate for states below the glass transition range also only at time scales exceeding the limits of human history”. Another critique was addressed to the flow behaviour of glasses as follows: “Because everything flows on such historical time scales, this feature is not a specific property of glasses and cannot be used to distinguish it from any other states of matter”.

As regards crystallization of glasses, it was pointed out [18] that intensive nucleation occurs in a relatively small range of temperatures (with a maximum close to  $T_g$ ) while the kinetic factor is correlated with viscosity, which significantly increases as temperature decreases. Therefore, perceptible crystal nucleation (i.e., devitrification) does not occur for a variety of glasses under normal conditions on the Earth. Assuming that local nucleation processes do proceed, this does not necessarily lead to full crystallization of the material, since the maximum growth rate is typically located at much higher temperatures [18].

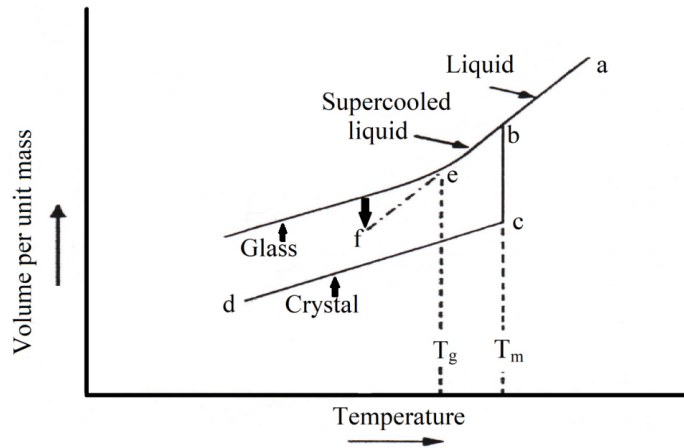


**Fig. 1.** Relation between the glassy, liquid and solid states:  $T_m$  - melting point or liquidus temperature,  $T_g$  - glass transition temperature. Dotted line e-f is the extrapolated line for the equilibrium liquid.

Thermal analysis methods, including differential thermal analysis (DTA), differential scanning calorimetry (DSC) and dilatometry, are commonly used to evaluate  $T_g$  since rearrangements that occur at glass transition lead to characteristic jumps of derivative thermodynamic parameters such as the specific heat or the coefficient of thermal expansion [19]. However, the values of  $T_g$  obtained by different techniques (e.g. from thermal analysis plots or thermal expansion curves) are not identical. Furthermore, the value of  $T_g$  depends on the heating rate applied to obtain those curves. Therefore,  $T_g$  is interpreted as the approximate temperature at which the supercooled liquid converts to a solid upon cooling, or, conversely, at which the glass starts behaving as a viscoelastic solid upon heating [5,6,11].

## 2 Theories of glass formation

Different cooling rates may be needed to form glasses in different compositional systems. Such experimental observation is behind several attempts to produce an atomic theory of glass formation based on the nature of the chemical bonds and the shape of the structural units involved. Although proposing a structural theory might seem contradictory for a material that is characterized by no long-range, periodic atomic order, some forms of short-range order allow reproducing the same glass from a nominal composition and reliably controlling the overall properties.

Two main approaches [5] were developed to explain glass formation: (i) the structural theories of glass formation, based on structural considerations such as geometry, nature of bond forces, etc., and (ii) kinetic approach, focused on controlling glass formation by changes in processing.

Inorganic glasses are readily formed from a wide variety of precursors, mainly oxides, chalcogenides, halides, salts, and their relevant combinations. There have been many attempts to relate the glass-forming tendency of a material to its molecular level structure. One of the earliest structural concepts was proposed in the 1920s by Goldschmidt [20] who suggested that the ability of an oxide to form a glass might be related to the way in which the oxygen ions were arranged around the cation to form the unit cell of the crystal structure. It can be shown from geometrical considerations that, for an oxide  $M_xO_y$ , the coordination number of the cation  $M$  is 4 if the ratio of ionic radii  $R_M/R_O$  lies approximately within 0.2-0.4. Goldschmidt observed that some glass-forming oxides (e.g.  $SiO_2$ ,  $GeO_2$  and  $P_2O_5$ ) typically exhibit a tetrahedral arrangement in the crystalline state and suggested that this might be a criterion of glass-forming ability. However, this theory was later found to be incomplete, being unable to adequately explain a variety of systems. In this regard, although all ionic glass formers satisfy Goldschmidt's rule, there are many systems that satisfy it but are not glass formers (e.g.,  $BeO$  and most halides).

In the early 1930s, Zachariasen [21] formulated the famous random network theory, according to which glass formers are cations that have high valences ( $\geq 3$ ) and can create three-dimensional networks of polyhedra. For instance, in silicate glasses, oxygen networks are formed by polymerization of polyhedra. By postulating that the oxygen polyhedra found in the oxide crystals would also be present in the glasses, Zachariasen introduced the concept of a continuous random network structure for a glass, where periodic structural arrangement is prevented by random orientations. He proposed that the structure of glass was similar to that of a crystal but with a larger lattice energy resulting from the disordered arrangements of polyhedral units, yielding a random network that lacks long-range periodicity (as shown schematically in Fig. 2). This was also demonstrated by the absence of sharp X-ray diffraction lines for glasses, the pattern of which is typically characterized by a broad halo. According to his experiments, Zachariasen suggested four rules for a structure to favour glass formation:

1. no oxygen atom must be linked to more than two cations;
2. the number of oxygen atoms surrounding any given cation must be small (typically 3 or 4);
3. oxygen polyhedra can share only corners, not edges or faces;
4. at least three corners of each oxygen polyhedron must be shared with other polyhedral.

The condition no. 4 was specifically introduced to ensure that the network would be three-dimensional (although certain glasses can exist in structures describable in fewer dimensions).

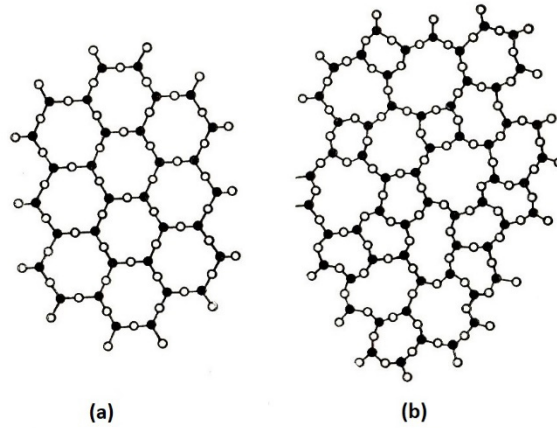


**Fig. 2.** Schematic representation of a two dimensional structure for (a) crystalline silica and (b) vitreous (glassy) silica (legend for both pictures: silicon – ● and oxygen –○). A fourth oxygen would be located above each cation in the three-dimensional structures.

These four rules lead to the open structures that can accommodate a distribution of inter-polyhedral bond angles which are associated with the loss of long-range structural order when a crystal forms a glass. Zachariasen concluded that oxides such as  $\text{SiO}_2$ ,  $\text{B}_2\text{O}_3$ ,  $\text{GeO}_2$ ,  $\text{P}_2\text{O}_5$  and  $\text{As}_2\text{O}_3$  are glass formers because oxygen coordination number for them is 3 or 4, which indicates that they can easily build up a characteristic network structure consisting of triangular or tetrahedral units. Diffraction studies made by Warren [22] and later by Wright [23] confirmed Zachariasen's prediction that glasses and crystals have similar short-range polyhedral structures but different long-range polyhedral arrangements. The Dietzel's field strength consideration (i.e.  $Z/a^2$  ratio, where  $Z$  is the charge of the cations and  $a$  is the cation-oxygen distance) represented an extension of the Zachariasen's network theory [7].

Along with the development of the random network hypothesis, the Lebedev's crystallite theory was also developed and adapted by a great number of glass researchers. According to Lebedev, silicate glasses are composed of assemblages of microcrystalline clusters of  $\text{SiO}_2$ , called crystallites [7].

The basic concepts of glass structural theories proposed by Zachariasen and Lebedev have been subjected to certain modifications which brought them closer to each other, but they still remained basically different [7].

Jiang and Zhang proposed a phase diagram model to explain various glass structures [24] and pointed out that neither the "random network" theory nor the "crystallite" hypothesis is a universal structural model for glass. Based on measurements from infrared spectroscopy, Raman and nuclear magnetic resonance (NMR), as well as the physical properties of relevant compounds in phase diagrams (e.g. density and refractive index), Jiang and Zhang concluded that glasses and crystalline congruent compounds exhibit similar NMR data and spectral features in a phase diagram. In their phase diagram structural approach, binary glass is considered to be a mixture of the

melts of the two nearest congruent compounds in a binary phase diagram; similarly, ternary glass is composed of a mixture of the three nearest congruent compounds in a ternary phase diagram. The structures and properties of the resulting glass can be predicted and calculated from the relevant characteristics of either two or three congruent compounds [24].

Other theories have also been proposed for predicting the easiness of glass formation based on some known data, such as the bonding strength between the constituent elements, the electronegativity values and the existence of deep eutectics in the phase diagrams [5]. Specifically, Shelby [5] proposed the fundamental law of structural models as a further guide to the testing of any complete structural model for glasses, which should take into account: (i) coordination number of all network cations, (ii) distribution of bond angles and rotations, (iii) connectivity of all network units, (iv) dimensionality of the network, (v) nature of any intermediate range order, (vi) morphology, (vii) bonding characteristics (field strength, bond strength, site specific bonding), (viii) nature of the interstitial or free volume, (ix) role of minor constituents, impurities and defects. However, a limitation of structural approaches is that they are unable to take into account the thermal history of the melt [20,21].

Especially in glass industry, special attention is addressed to the purification of the glass compositions from impurities and mineralisers which might promote crystal nucleation and, thus, unwanted devitrification. Multiple melting cycles, superheating and centrifugation are typically applied to avoid the effect of impurities on nucleation, in order to achieve solidification of liquid phases without undergoing crystallization at a quite considerable degree of supercooling [7].

Glass forming ability is defined in terms of resistance to crystallization of a melt upon cooling and varies with the variation in composition and size of the melt. Hence, the difference in glass forming ability of two closely related compositions can be provided by the kinetic approach to glass formation as discussed by Shelby [5]. A similar concept to glass forming ability is glass stability, which can also be thought in terms of glass resistance to crystallization. Glass stability is often quantified by the difference in temperature between the onset of crystallization ( $T_c$ ) and  $T_g$  for a sample heated at a specific linear rate (i.e.,  $T_c - T_g$ ). Alternatively, the temperature of the first maximum or peak ( $T_p$ ) in the DTA or DSC plot can be considered instead of  $T_c$  to calculate this temperature difference [5].

In the 1970s, Hrubý [25, 26] proposed another parameter to measure glass stability, defined as:

$$K_H = (T_c - T_g)/(T_m - T_c) \quad (1)$$

According to Hrubý, the larger  $K_H$  of a certain glass, the greater its stability against crystallization upon heating.

Turnbull and Cohen [27] proposed the determination of kinetic stability on cooling experiments through the steady-state nucleation rate. Gutzow et al. [2] related the glass stability to the non-steady-state time lag,  $\tau$ . These kinetic approaches assume that one of the three considered parameters, i.e. crystal nucleation rate, crystal growth rate or  $\tau$ , is dominant over the other two, the contributions of which can be accordingly neglected [28]. Uhlmann et al. [29] considered crystal nucleation and growth rate simultaneously, formulating a kinetic criterion for vitrification; the kinetic theory of glass formation was extended to include non-steady state effects and heterogeneous nucleation. Weinberg et al. [30,31] found that the volume fractions transformed and

the resulting critical cooling rates ( $R_c$ ) are quite sensitive to the method of calculation. For instance, the nose method based on isothermal Time-Temperature-Transformation (TTT) curves overestimates  $R_c$  by up to one order of magnitude. It was also demonstrated that  $R_c$  is highly sensitive to the main physical properties dictating the nucleation and growth kinetics, i.e. crystal liquid surface energy, thermodynamic driving force and viscosity [32]. Weinberg [33] also integrated the equation of overall crystallization kinetics to estimate and compare the criteria for vitrification on cooling and glass stability against crystallization on heating, and apparently concluded that glass forming ability and glass stability are, surprisingly, ill-related concepts.

Using experimental values of crystal nucleation and growth rates for four glasses that nucleate in the bulk, Cabral et al. [34] calculated the critical cooling rates for glass formation ( $R_c$ ) by the TTT method. It was shown a correlation between the Hrubý parameter of glass stability ( $K_H$ ) and glass forming ability. Avramov et al. [28] repeated and extended the calculations initially done by Weinberg [33] and demonstrated that glass forming ability and glass stability are indeed directly related quantities, as already suggested by the experimental results reported by Cabral et al. [34].

Glass stability against crystallization deserves to be taken into account not only during the initial melting procedure of the material but also when massive glass products need to be fabricated, for example, by applying high-temperature treatments on glass powder compacts well above  $T_g$  (sintering). It is well known that viscous flow sintering of glass particles can effectively occur when the surface tension is high and the viscosity is low, i.e. when the glass shows its lower viscosity, without undergoing any crystallization process [35,36]. Lara et al. [37] introduced a parameter that quantifies the sinterability of glass, defined as:

$$S_c = T_c - T_{MS} \quad (2)$$

where  $T_{MS}$  is the temperature of maximum shrinkage determined from hot-stage microscopy (HSM).

This parameter measures the competition between glass sintering and crystallization that concurrently occur during heating (sinter-crystallization). The temperature difference between onset of crystallization and maximum shrinkage (i.e., densification) is a measure of the ability of sintering versus crystallization: in other words, the greater  $S_c$ , the more independent the kinetics of the two processes. A general rule can be proposed for the interpretation of  $S_c$ : if  $S_c < 0$ , only partial densification is achieved before crystallization begins; otherwise, if  $S_c \geq 0$ , full densification occurs prior to crystallization [38]. Therefore, higher values of  $S_c$  are related to higher final densities, which indicate a better sintering behaviour leading to a more efficient densification of the final glass sample. Other details on these topics are provided in the section 7.

### 3 Methods for glass production: an overview

The glasses used over most of our history have been silicate glasses traditionally formed by cooling from a melt. Glass processing by melting comprises four main steps: (i) batch preparation, (ii) melting, (iii) fining and (iv) homogenization. Batch preparation involves the selection of raw materials, batch calculation (i.e. assessing the amounts of precursors to achieve a given glass composition), weighing and mix-

ing these materials to get homogeneous starting batch. A series of transformations occur during the conversion of a batch, usually composed by solid powders of oxides, carbonates and other salts, to a melt upon heating, including the release of physically-adsorbed and chemically-bonded water, solid state reactions with formation of double carbonates such as  $\text{Na}_2\text{Ca}(\text{CO}_3)_2$  and  $\text{CaMg}(\text{CO}_3)_2$ , thermal decomposition of carbonates, sulphates and nitrates, liquid phase formation (e.g. due to melting of eutectic mixtures or melting of some substances). Further heating leads to the increase in volume fraction of a liquid phase, synthesis of new compounds such as silicates (e.g.  $\text{Na}_2\text{SiO}_3$ ,  $\text{Ca}_2\text{SiO}_4$ ,  $\text{Na}_2\text{O}\cdot 3\text{CaO}\cdot 6\text{SiO}_2$ ) and aluminates (e.g.  $\text{Na}_2\text{Al}_2\text{O}_4$ ,  $\text{CaAl}_2\text{O}_4$ ), dissolution of refractory components such as silica and alumina in the liquid phase. Removal of gas bubbles (i.e. fining) is usually required in order to reduce the heterogeneity of the melt; furthermore, these gaseous inclusions are unwanted in commercial products due to both antiesthetic and functional reasons (internal pores reduce mechanical performance and can be the trigger for crack propagation). Then, additional time for diffusion processes and creation of convection flow via stirring in the melt is usually needed to convert the melt to a homogeneous liquid; gas bubbling through the melt can be performed at this stage if obtaining glass foams is the goal. The melting temperature varies depending on the glass composition: common silica-soda-lime glasses typically require above  $1400^\circ\text{C}$  to be melted, but phosphate glasses can be produced at significantly lower temperatures (even below  $1000^\circ\text{C}$  in some cases).

In order to obtain glass products of desired shape and size, the melt can be poured into molds replicating the negative of the object. Alternatively, the melt can be quenched into water to obtain a “frit”, which is composed by small chunks of glass that are thermally-shocked and reduced in fine pieces; this approach is very useful in the production of glass powder for further processing (e.g. milling followed by pressing or coating and final sintering). Glass fibers can also be drawn starting from a melt-derived glass cylinder (“preform”) heated within a specific temperature range above  $T_g$  by using a proper equipment (drawing tower).

Melting is indeed the most common, easy and relatively quick method to produce glass and is widely used for commercial mass-production. However, if high purity of the final product is a major goal, glass can also be synthesized via a “wet” method, i.e. the sol-gel process. Sol-gel silicate glasses are inherently nanoporous (or, more specifically, mesoporous) materials (pore size within 2-50 nm) exhibiting a larger specific surface area (well above  $50 \text{ m}^2/\text{g}$ ) as compared to melt-derived glass of analogous composition (specific surface area less than  $1 \text{ m}^2/\text{g}$ ) [39,40]. The sol-gel method is classified as a chemistry-based synthesis route in which the polymerization reactions in a colloidal suspension (sol) containing appropriate precursors of glass oxides leads to sol gelation at room temperature. Sol-gel glasses are usually produced by hydrolysis and poly-condensation of alkoxide precursors (e.g. tetraethyl orthosilicate (TEOS) or tetramethyl orthosilicate (TMOS)) followed by aging and drying under ambient atmosphere. The precursors of other oxides (e.g. CaO) are introduced in the sol by adding and solubilizing appropriate salts (e.g. calcium nitrate decahydrate). The overall sol-gel process can be divided in 5 major steps. During step 1, liquid and solid reagents are mixed together at room temperature to induce the formation of covalent bonds between the elements. Hydrolysis and poly-condensation occur simulta-

neously while the sol undergoes homogenization. Then, during gelation at room temperature (step 2), viscosity increases due to the formation of a three-dimensional interconnected network. Poly-condensation continues during aging at around 60°C (step 3) and is accompanied by decrease in porosity and improvement in mechanical strength. Both these aspects are fundamental to avoid cracking during drying (step 4), which is typically performed at 120 to 150°C to eliminate the liquid phase from the pores. The dried gel is then stabilized by high-temperature thermal treatment in the range of 500 to 700 °C (step 5), which is lower than the melting temperature typically required to produce melt-derived silicate glasses. The major limitations of sol-gel approach compared to melting route include the long time required for the whole synthesis (several days), the poor mechanical properties of the final glass monolith due to inherent nanoporosity, and the need for a careful control on the synthesis parameters (e.g. pH, environmental temperature) which can deeply affect the properties of the final product (homogeneity, phase segregation during the synthesis, crystallization).

At present, inorganic glasses can be produced starting from many compositions based on silica, phosphorus oxide, boron oxides, halides or chalcogenides. However, silicate glasses are the most important regarding commercial impacts because they typically have excellent transparency, good chemical durability and can be produced by using inexpensive natural precursors.

#### **4 The role of oxides on glass structure, properties and glassmaking**

According to the random network theory, Zachariasen [21] introduced the basis for the most commonly-used models for glass structures. Depending on the role in glass production, oxides are usually classified in three groups: (i) network formers, such as  $\text{SiO}_2$ ,  $\text{B}_2\text{O}_3$ ,  $\text{P}_2\text{O}_5$ , having oxygen coordination numbers equal to 3 or 4 and tending to produce the basic cross-linked “polymeric” glass structure; (ii) network modifiers, which typically are alkaline and alkaline-earth oxides such as  $\text{Na}_2\text{O}$ ,  $\text{K}_2\text{O}$  and  $\text{CaO}$ , having coordination number equal to 6 or more and generally tending to reduce the degree of polymerization and viscosity; and (iii) intermediate oxides, with metallic cations such as  $\text{Al}^{3+}$ ,  $\text{Zn}^{2+}$ ,  $\text{Pb}^{2+}$  and  $\text{Ti}^{4+}$ , having intermediate coordination of 4 to 6 and acting either as network formers or modifiers, depending on the glass composition [5,12,41].

Oxides with high coordination numbers and relatively weak bonds (i.e., the network modifiers) alter the glass-forming network by replacing stronger bridging oxygen (BO) bonds between glass-forming polyhedra with weaker, non-bridging oxygen (NBO) bonds, thereby modifying the polyhedral structure [5]. Fig. 3 shows a schematic 2D representation of the random network of an alkali-silicate glass. The network modifiers are important constituents in most technological glasses because they are useful to decrease the melting temperature, with an obvious impact on energy consumption and related costs, and control many properties, such as chemical stability. Modifiers are commonly used to facilitate the glass production at lower temperatures because they promote the viscosity decrease by disrupting the network of the

glass melt [12]. Silica glass (without any modifiers) is difficult to process because its melting temperature is about 1713 °C, which corresponds to cristobalite-liquid equilibrium. If 25 wt.% of Na<sub>2</sub>O is added to SiO<sub>2</sub>, the liquidus temperature is lowered to only about 793 °C, which is a significant advantage from a technological viewpoint [42]. Alkaline metal ions (e.g. Na<sup>+</sup>) are monovalent, mobile and allow ion migration while alkaline-earth ions, being typically bivalent (e.g. Ca<sup>2+</sup>) and thus electrically compensated by two NBOs, are relatively immobile and can hinder the diffusion of other ions, especially the alkaline ones, thus improving the chemical resistance of the glass [12]. For this reason, most of important commercial glasses are based on silica-soda-lime compositions comprising SiO<sub>2</sub> (network former), Na<sub>2</sub>O and CaO (alkaline and alkaline-earth modifiers, respectively).

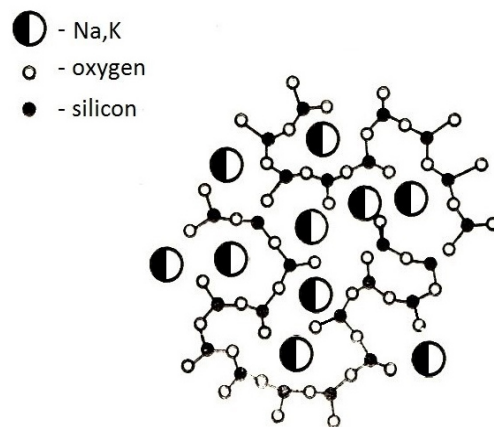


**Fig. 3.** Schematic representation of atomic arrangement in an alkali-silicate glass. A fourth oxygen would be located above each cation in the three-dimensional structure.

Intermediates such as Al<sub>2</sub>O<sub>3</sub>, WO<sub>3</sub>, TiO<sub>2</sub>, ZrO<sub>2</sub> and SeO<sub>2</sub> can link the continuous network or locally replace cations of formers (e.g. Si<sup>4+</sup> with Al<sup>3+</sup>), but are unable to form a glass network by themselves. Introducing Al<sub>2</sub>O<sub>3</sub> in a silicate glass can yield better mechanical properties (hardness, strength and elastic modulus) as well as higher chemical stability and durability of the material.

The relative concentration of BO and NBO plays a key role on the structure and properties of glasses [43]. According to the number of BO in a tetrahedral unit of silicate glasses, the following scenarios can be considered:

1. BO = 4 (i.e. [O]/[Si] = 2): each BO is shared by two silicon atoms and the network is three-dimensional with all four corners bridging;
2. BO = 3 (i.e. [O]/[Si] = 2.5), the network is two-dimensional with three corners bridging (note that some tetrahedra may be linked to four others and some therefore to less than three, the said number being the average value over the network);
3. BO = 2 (i.e. [O]/[Si] = 3), the network is formed by one-dimensional chains with one corner bridging;

4.  $BO < 2$  (i.e.  $[O]/[Si] > 3$ ), the network is composed of individual  $SiO_4$  tetrahedral units, some of them being bound together.

The rigidity of the glass network gradually decreases by replacing BO with NBO until only individual isolated tetrahedra remain. The notation  $Q^n$  is usually preferred among glass scientists, where  $n$  is the number of BO in a tetrahedron; accordingly, it is possible to refer to (1)  $Q^4$ , (2)  $Q^3$ , (3)  $Q^2$  and (4)  $Q^1$  or  $Q^0$  structures, respectively.

Considering an oxide glass of general composition  $(A_2O)_x(SiO_2)_{1-x}$ , where  $A$  is the alkaline metal, if  $x = 0$  (i.e. pure silica) only BO exist ( $Q^4$ ); if the alkali concentration increases, a dramatic decrease of BO and an increase of NBO occur accordingly [12]. The intermediate oxides have coordination numbers and bond strengths between the network formers and network modifiers and tend to have an intermediate effect on glass properties [44].

In the case of oxide glasses, the short-range structure can be extremely well-defined in terms of the coordination polyhedra of the network-forming cation such as silicon. These glasses are characterized by predominantly heteropolar bonding between network-forming cations and oxygens. Bond lengths and angles in the first coordination shell of oxygens around these cations vary only over a narrow range. Glass-forming cation-oxygen polyhedra, like  $SiO_4$  units, are usually corner-linked through BO and form a three-dimensional connected network. The properties of glasses mainly rely on its structure which, in the case of silica glass, consists of well-defined  $SiO_4$  tetrahedra connected to another neighbouring tetrahedron through each corner (Fig. 2b). Neutron diffraction studies revealed that the Si–O distance in the tetrahedron is about 0.16 nm and the shortest O–O distance is about 0.26 nm, which are the same dimensions as found in crystalline silica (quartz). The inter-tetrahedral (Si–O–Si) bond angle distribution is centred around  $143^\circ$  but is much broader than that found in crystalline silica, thus producing the loss in long-range order already shown in Fig. 2b [23,45].

Similarly to pure-silica glass, the structure of alkali-silicate glasses also consists of a network of  $SiO_4$  tetrahedra, but some of the corners are now occupied by NBO that are linked to the modified polyhedra (Fig. 3). Increasing the concentration of modifiers leads to increasing the relative fraction of NBO associated with the glass network, which leads to reducing  $T_g$  and melt viscosity as well as increasing the thermal expansion coefficient and ionic conductivity [46].

The changes in the silicate glass network, and hence the compositional dependence of many of the glass properties, can be described by taking into account the relative fractions of BO and NBO or, alternatively, the concentrations of the different  $Q^n$  units [12]. The rigidity of the network decreases gradually by replacing BO by NBO until only individual isolated tetrahedra remain ( $Q^0$ ). Glasses containing less than 10 mol.% of alkaline oxides are considerably more difficult to melt due to high viscosity [5]. Moreover, alkali-deficient glasses are prone to phase separation and devitrification on a scale of 0.1-1  $\mu m$  [46]. Modifiers disrupt the network and are used to lower the viscosity of the glass melt and, hence, to facilitate glass production at lower temperatures.

The viscosity-temperature relationship is one of the key point in determining the easiness of glass formation of any melt. Glass formation is favored when crystallization is discouraged by the kinetic barrier to atomic arrangement, provided that (i) the

viscosity is very high at the melting temperature of the crystalline phase which would form from the melt and/or (ii) the viscosity increases very rapidly as temperature decreases [5]. In commercial glasses, melting usually takes place at a viscosity of  $\leq 10$  Pa·s and the viscosity at working point (i.e. when a glass object is delivered to processing/shaping) is about  $10^3$  Pa·s. The softening point corresponds to the value of viscosity that is sufficiently high to prevent deformation under glass' own weight, while the temperature range between the working point and softening point is referred as the working range: melts that demonstrated a wide working range are called as "long glasses" and those with a short working range are known as "short glasses". As soon as a glass object is formed, it is subjected to annealing to release internal stresses: the annealing point typically corresponds to a viscosity range of  $10^{12}$  to  $10^{12.4}$  Pa·s and is defined as the temperature at which the stress is substantially relieved in a few minutes [5].

It cannot be ignored that some glass formulations that are being cooled to a temperature suitable for forming may partially devitrify, thus developing small crystals embedded in the amorphous matrix. In order to avoid this unwanted phenomenon during glass manufacturing processes, the glass composition should be designed so that the temperature interval of crystallization is narrow, the rate of crystal growth is low and the  $T_p$  value is significantly higher than glass-working temperature.

In many systems, the region of glass formation coincides with a region of the phase diagram where the liquidus temperature is low. The silica-soda-lime ( $\text{SiO}_2$ - $\text{Na}_2\text{O}$ - $\text{CaO}$ ) system, which is very common in glass technology, might serve as an instructive example [47]. Morey and Bowen [48] studied the phase relations of the pseudo-binary system  $\text{CaO}\cdot\text{SiO}_2$ - $\text{Na}_2\text{O}\cdot\text{SiO}_2$ . Later Morey [49] investigated the phase equilibria in the silica-rich region ( $>50$  wt.% of  $\text{SiO}_2$ ) of the  $\text{CaO}\cdot\text{SiO}_2$ - $\text{Na}_2\text{O}\cdot\text{SiO}_2$  system in greater detail. Morey and Bowen found four ternary compounds:  $\text{Na}_2\text{O}\cdot 3\text{CaO}\cdot 6\text{SiO}_2$  (devitrite),  $\text{Na}_2\text{O}\cdot 2\text{CaO}\cdot 3\text{SiO}_2$ ,  $2\text{Na}_2\text{O}\cdot \text{CaO}\cdot 3\text{SiO}_2$  and  $\text{Na}_2\text{O}\cdot \text{CaO}\cdot \text{SiO}_2$ . Fig. 4 shows the silica-rich region of the silica-soda-lime phase diagram according to Morey and Bowen [48,49].

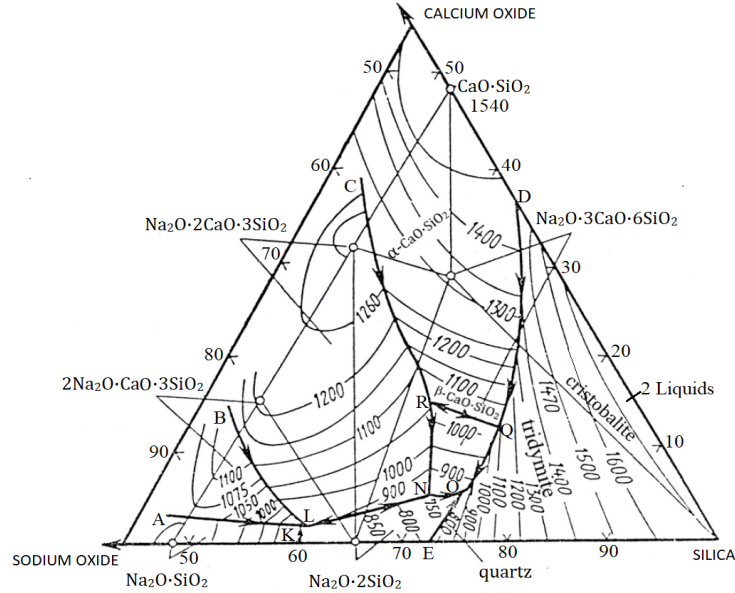


**Fig. 4.** Silica-rich region of the silica-soda-lime phase diagram (in wt.%) [48,49].

New compounds, i.e.  $4\text{Na}_2\text{O}\cdot 3\text{CaO}\cdot 5\text{SiO}_2$  and  $\text{Na}_2\text{O}\cdot 2\text{CaO}\cdot 2\text{SiO}_2$ , were reported by Segnit [50] who studied the  $(\text{CaO}, \text{Na}_2\text{O})$ -rich part of the system and showed that  $\text{Na}_2\text{O}$  forms solid solutions with dicalcium silicate. Toropov and Arakelyan investigated two compounds,  $2\text{Na}_2\text{O}\cdot 8\text{CaO}\cdot 5\text{SiO}_2$  and  $2\text{Na}_2\text{O}\cdot 4\text{CaO}\cdot 3\text{SiO}_2$ , and demonstrated that they are solid solutions of alkali-silicates in calcium orthosilicate [51]. Table 1 collects the invariant points of the system according to Morey and Bowen [48,49].

**Table 1.** Invariant points in the  $\text{SiO}_2$ - $\text{Na}_2\text{O}$ - $\text{CaO}$  system (see Fig. 4).

Relevant points in the diagram	Equilibrium phases	Process	Composition (wt.%)			Temperature (°C)
			$\text{Na}_2\text{O}$	$\text{CaO}$	$\text{SiO}_2$	
(K)	$\text{Na}_2\text{O}\cdot 2\text{SiO}_2 + \text{Na}_2\text{O}\cdot \text{SiO}_2 + 2\text{Na}_2\text{O}\cdot \text{CaO}\cdot 3\text{SiO}_2 + \text{L}$	eutectic	37.5	1.8	60.7	821
(L)	$2\text{Na}_2\text{O}\cdot \text{CaO}\cdot 3\text{SiO}_2 + \text{Na}_2\text{O}\cdot 2\text{CaO}\cdot 3\text{SiO}_2 + \text{Na}_2\text{O}\cdot 2\text{SiO}_2 + \text{L}$	tributary reaction point	36.6	2.0	61.4	827
(N)	$\text{Na}_2\text{O}\cdot 2\text{SiO}_2 + \text{Na}_2\text{O}\cdot 2\text{CaO}\cdot 3\text{SiO}_2 + \text{Na}_2\text{O}\cdot 3\text{CaO}\cdot 6\text{SiO}_2 + \text{L}$	tributary reaction point	24.1	5.2	70.7	740

(O)	$\text{Na}_2\text{O}\cdot 3\text{CaO}\cdot 6\text{SiO}_2 +$ $\text{Na}_2\text{O}\cdot 2\text{SiO}_2 + \text{SiO}_2 + \text{L}$	eutectic	21.3	5.2	73.5	725
(Q)	$\text{SiO}_2 + \text{CaO}\cdot \text{SiO}_2 +$ $\text{Na}_2\text{O}\cdot 3\text{CaO}\cdot 6\text{SiO}_2 + \text{L}$	tributary reaction point	13.7	12.9	73.4	1035
(R)	$\text{Na}_2\text{O}\cdot 3\text{CaO}\cdot 6\text{SiO}_2 +$ $\text{Na}_2\text{O}\cdot 2\text{CaO}\cdot 3\text{SiO}_2 +$ $\text{CaO}\cdot \text{SiO}_2 + \text{L}$	tributary reaction point	19.0	14.5	66.5	1030

The ternary eutectic point at which quartz coexists with  $\text{Na}_2\text{O}\cdot 3\text{CaO}\cdot 6\text{SiO}_2$ ,  $\text{Na}_2\text{O}\cdot 2\text{SiO}_2$  and liquid was established to be at 725 °C. The ternary  $\text{SiO}_2$ - $\text{Na}_2\text{O}$ - $\text{CaO}$  diagram is the basic phase diagram for commercial glass compositions with  $\text{SiO}_2$ ,  $\text{Na}_2\text{O}$  and  $\text{CaO}$  as major constituents and can also be used to describe, under certain approximations, multicomponent glass systems with some additional oxides (> 3) as minor constituents. Additional modifiers and intermediate may be required to finely modulate the glass forming ability and final properties. For example, addition of  $\text{Al}_2\text{O}_3$  increases the chemical resistance of the glass as well as the glass stability against crystallization due to the increase network connectivity. Essentially, introduction of  $\text{Al}_2\text{O}_3$  in a silicate network yields the substitution of  $\text{Si}^{4+}$  with  $\text{Al}^{3+}$  cations so that  $\text{AlO}_4$  tetrahedra join the network formed by  $\text{SiO}_4$  tetrahedra, provided that an additional  $\text{Na}^+$  cation occupies an interstitial hole in order to maintain charge neutrality.

Many of commercial glass compositions (Table 2) are located in the region of primary phase formation of devitrite and wollastonite, i.e. inside the triangle with the vertexes corresponding to the compounds  $\text{Na}_2\text{O}\cdot 2\text{SiO}_2$ ,  $\text{Na}_2\text{O}\cdot 3\text{CaO}\cdot 6\text{SiO}_2$  and  $\text{SiO}_2$ . All the melts with the compositions located in that triangle will solidify in the ternary eutectic with composition 21.3 wt.%  $\text{Na}_2\text{O}$ , 5.2 wt.%  $\text{CaO}$  and 73.5 wt.%  $\text{SiO}_2$  at 725 °C (i.e. in the point “O” in Fig. 4).

**Table 2.** Representative commercial glass compositions (wt.%) [47].

Type of glass	$\text{SiO}_2$	$\text{CaO}$	$\text{MgO}$	$\text{Na}_2\text{O}$	$\text{K}_2\text{O}$	$\text{Al}_2\text{O}_3$
Window	71	10	3	14	1	1
Food container	72	3	7.5	15	1	1.5
Plate	71	11	4	13	-	1

Resistance to crystallization can also be improved when  $\text{CaO}$  is partially substituted by  $\text{MgO}$  in  $\text{SiO}_2$ - $\text{Na}_2\text{O}$ - $\text{CaO}$  glasses [52]. This is demonstrated by the data reported

in Table 3: for example, looking at the glasses containing 18 wt.% of Na<sub>2</sub>O (compositions from no. 19 to 24), one can see that the decrease in CaO content from 16 to 8 wt.%, which is accompanied with an equivalent increment in MgO, leads to a significant decrease in maximum crystal growth rate from 200 to 5  $\mu\text{m}/\text{min}$ . Similar trends can also be observed for the other compositions listed in Table 3.

**Table 3.** Compositional effect on resistance to crystallization [52]

Composition no.	Na <sub>2</sub> O/CaO weight ratio	Crystallization range (°C)	Maximum crystal growth rate, ( $\mu\text{m}/\text{min}$ )	Crystalline phases formed
1.	12/6	800-1350	90	Quartz
2.	12/8	800-1300	60	Quartz
3.	12/10	900-1250	40	Quartz
4.	12/12	750-1000	30	Devitrite
5.	12/14	850-1150	15	Devitrite, Quartz
6.	12/16	900-1100	38	Devitrite, Quartz
7.	14/6	900-1200	50	Quartz
8.	14/8	900-1200	40	Quartz
9.	14/10	850-1200	30	Devitrite, Quartz
10.	14/12	900-1050	10	Devitrite
11.	14/14	800-1100	37	Devitrite, Quartz
12.	14/16	800-1100	70	Devitrite, Quartz, Wollastonite
13.	16/6	950-1150	35	Quartz
14.	16/8	900-1100	10	Quartz
15.	16/10	800-1000	10	Quartz
16.	16/12	800-1000	20	Devitrite, Quartz
17.	16/14	800-1000	75	Devitrite
18.	16/16	800-1000	70	Devitrite, pseudo-Wollastonite
19.	18/6	800-1000	10	Wollastonite
20.	18/8	800-950	5	Quartz
21.	18/10	850-950	5	Quartz
22.	18/12	800-1000	30	Devitrite, Quartz
23.	18/14	800-1100	100	Devitrite
24.	18/16	800-1100	200	Devitrite, pseudo-Wollastonite

Chemical composition of glasses is determined by the type of raw materials used to prepare a batch. Glasses are either produced from high-quality, chemically pure components or from a mixture of less pure materials [5]. While glasses for research and high-tech applications are typically produced from expensive, high-purity chemicals, bulk commercial glasses are produced mostly from natural materials. Specifically,

alkaline, alkaline-earth oxides and silica are usually introduced through using soda ash, potash, nepheline syenite, calcite, dolomite, magnesite, and silica sand, which may contain some impurities such as  $\text{Fe}_2\text{O}_3$ ,  $\text{TiO}_2$ ,  $\text{Mn}_2\text{O}_3$ ,  $\text{MnO}_2$  and  $\text{Cr}_2\text{O}_3$ . Therefore, a complete chemical analysis of the glass could reveal not only major (i.e.  $\text{SiO}_2$ ,  $\text{Na}_2\text{O}$ ,  $\text{CaO}$ ) and minor constituents (e.g.  $\text{K}_2\text{O}$ ,  $\text{MgO}$  and  $\text{Al}_2\text{O}_3$ ), but non-negligible traces of impurities. In order to approximate the composition to a ternary system, the major constituents might be arranged into 3 groups, i.e. alkali oxides (from monovalent cations), alkaline-earth oxides (from bivalent cations) and glass formers (silica and others) [47]: compositions having 72-74 wt.% of glass formers and 26-28 wt.% of alkaline/alkaline-earth oxides which are located near the upper area of the boundary OQ in Fig. 4 exhibit improved glass stability and high chemical resistance [52].

Most glasses for both common and high-tech applications are based on silicate systems, which may also incorporate small amounts of other formers. However, glasses having other major formers have shown great suitability for special applications, such as borate glasses in biomedicine and phosphate glasses in optics; these topics will be discussed in dedicated chapters of this book.

## 5 From glasses to glass-ceramics: a short historical overview

It has been known for a long time that glasses can be crystallized to form polycrystalline ceramics. One of the early evidences of this knowledge, initially relying on an empirical basis than on a clear theoretical background, dates back to the 3<sup>rd</sup> century AD. Chemical and microstructural analyses carried out on mosaic tesserae of the Roman Age revealed that the white colour of these archaeological materials was due to the presence of crystalline phases nucleated and grown in the glass matrix as a consequence of a thermal treatment. It was supposed that Roman craftsmen bought relatively cheap and transparent silica-soda-lime glass and, in a second manufacturing step, deliberately heat-treated this colourless material to convert it to a glass-ceramic to be used in the final form of opaque white tesserae [53].

Apparently, this knowledge was lost during the Medieval Age and only after 14 centuries partially-crystallized glasses were produced again according to a controlled treatment. In the first half of the 18<sup>th</sup> century, René-Antoine Ferchault de Réaumur tested certain glass compositions such as cut glass, porcelain glazes, mirror and window glass in his series of novel experiments on porcelain production. In particular, hollow glass articles, filled with a mixture of silica sand and calcined gypsum and embedded in the same mixture of materials, were heat-treated at temperatures corresponding to red heat for above 24 hours [54,55]. In the course of the annealing process, the originally transparent glass changed into a white stone-like product, which was visually very similar to porcelain. However, unlike conventional porcelain bodies, the new product possessed a high resistance to thermal shocks. The fracture surface of Réaumur's porcelain exhibited thin needle-like crystals grown from its periphery towards the center and embedded in a glass matrix [54]. Réaumur's porcelain was the first commercial material produced in the Modern Age by applying a roughly-standardized heat treatment on glass; it paved the way to future glass-ceramic production, although the crystallization process had not been fully controlled yet [10,11].

Two centuries later (around 1930), Becker [54] proposed the crystallization of  $4\text{Na}_2\text{O}\cdot 3\text{CaO}\cdot 10\text{SiO}_2$  glass to produce refractory vessels for glass and metal industries. A breakthrough in this field of research came out after the pioneering work of Donald Stookey at the Corning Glass Works (USA) when the theory of glass phase separation was proposed [56-58]. Glass-ceramics (GCs) were “formally” discovered in 1953 – and this was actually the third discovery, after the accidental discoveries made by ancient Roman craftsmen and Réaumur. However, also in this case the re-discovery of GCs was somewhat accidental. A sample of photosensitive lithium disilicate glass with precipitated silver particles was placed inside a furnace for undergoing heat treatment at 600 °C; however, a problem in the controller let the temperature to increase to 900 °C. Stookey expected to obtain a blob of melted glass and a ruined furnace, but he discovered that the lithium disilicate glass had transformed into a milky white plate. Another accident led to an extraordinary observation: when Stookey tried to remove it from the supporting substrate, the sample slipped from the tongs and bounced on the floor instead of shattering [59]. This phenomenon was explained further by formation of crystals in a matrix of glass, resulting in a GC material possessing properties of both glass and ceramics. Crystallization is the process by which well-ordered or regular periodic crystalline structures are produced from a non-periodic structure, like that of common glass [60,61]. In its simplest form, crystallization is observed when a melt of a single pure substance or compound is cooled. According to Tammann [60], the crystallization process is actually the sequence of two independent processes: (i) nucleation, which corresponds to the formation of crystallization centers and (ii) crystal growth from such centers. The theory of nucleation and crystal growth was expanded by Stookey to develop glass-ceramics in a controlled way [10]. He postulated that (i) almost all known glasses are metastable at room temperature as compared to the more thermodynamically-stable crystalline state and (ii), at least theoretically, they are prone to be crystallized provided that appropriate catalyst crystals are introduced into the melt [58]. Stookey literally said: “I am most proud of opening up a whole new field of science - the nucleation of crystallization of glass - that produced all kinds of new crystalline products with so many different useful properties” [56].

## 6 Production of glass-ceramics

Nucleation is the key factor for controlling crystallization in GCs. Crystal nuclei must be present in the glass matrix so that the crystal growth can start. Nucleation involves the formation of long-range atomic order regions (also called seeds or embryos), which are normally present in melted materials or in supercooled liquids. The embryos turn into nuclei when they attain a critical minimum size that makes them capable of spontaneously developing into large particles of the stable phase. This was initially observed in photosensitive glasses where noble metal crystallites serve as catalysts for the crystallization of lithium metasilicate crystals [58].

Two distinct types of nucleation can occur: (i) homogeneous nucleation or (ii) heterogeneous nucleation [5,10]. In the process of homogeneous nucleation, the first

small seeds have the same composition as the final crystals which will grow upon them, while in heterogeneous nucleation the nuclei are chemically different from the formed crystals. Homogeneous nucleation is believed to occur due to local fluctuations of density and kinetic energy in the absence of any foreign boundaries [10]. On the contrary, heterogeneous nucleation involves the presence of foreign boundaries such as substrates (external boundaries, for example in coatings) and grain boundaries (internal boundaries). Heterogeneous nucleation is also called catalyzed nucleation and is used for the development of most glass-ceramic systems. The theory of nucleation involves a thermodynamic parameter, known as Gibbs free energy ( $G$ ), which depends on other thermodynamic parameters: the enthalpy ( $H$ ), i.e. the internal energy of the system, and the entropy ( $S$ ), i.e. a measurement of the disorder of atoms or molecules in the system [5]. It is worth underlining that, from a thermodynamic viewpoint, a transformation occurs spontaneously only if  $G < 0$ .

Silicate GCs are the product of controlled crystallization of a  $\text{SiO}_2$ -based liquid between  $T_g$  and the melting point,  $T_m$ , of the major crystalline phase [61, 62]. GCs are usually obtained via two steps: first, a glass is formed by a conventional glass-manufacturing process; then, the glass product is shaped, cooled and reheated above  $T_g$ . The second step is sometimes repeated as a third step. A very fine-grain microstructure of GCs can be achieved by carefully selecting the crystal nucleation and growth conditions. Relatively coarse-grained GCs are produced during the direct cooling path of a melted viscous liquid; however, this method is seldom applied to induce and control internal crystallization.

Stookey mentioned that the efficiency of a given catalyst crystal depends on a number of factors, including the similarity between its crystal structure and that of the crystal phase to be nucleated [58]. He succeeded in achieving volume crystallization of the  $\text{Li}_2\text{O-K}_2\text{O-Al}_2\text{O}_3\text{-SiO}_2$  parent glass composition [10] by incorporating metal ions, such as  $\text{Ag}^+$ , acting as nucleation agents. The typical composition of the parent glass was 80  $\text{SiO}_2$ , 4  $\text{Al}_2\text{O}_3$ , 10.5  $\text{Li}_2\text{O}$ , 5.5  $\text{K}_2\text{O}$ , 0.02  $\text{CeO}_2$ , 0.04  $\text{AgCl}$  (wt.%) [10]. Under exposure to UV light,  $\text{Ce}^{3+}$  was oxidized to  $\text{Ce}^{4+}$  while metal ions were reduced to the atomic state (e.g.  $\text{Ce}^{3+} + \text{Au}^+ \rightarrow \text{Ce}^{4+} + \text{Au}^0$ ), thus forming heterogeneous nuclei for crystallization of lithium metasilicate during subsequent heat treatment. Lithium metasilicate easily dissolves in dilute HF, thus allowing high-precision patterned GCs to be prepared: this was the case of commercial Fotoform<sup>®</sup>, which is useful in fluidic devices, display screens, lens arrays, magnetic recording head pads, charged plates for inkjet printing and other high-tech devices [63]. Fotoceram<sup>®</sup>, having  $\text{Li}_2\text{Si}_2\text{O}_5$  and quartz as crystalline phases, was the commercial evolution of Fotoform<sup>®</sup>. A more comprehensive overview of the physics of nucleation can be found in Höland and Beall's book on glass-ceramics [10] as well as in Borrelli's book on photosensitive glasses and glass-ceramics [64].

The fundamental research carried out by Stookey stimulated further advances related to GC development while nucleating agents such as fluorides,  $\text{ZrO}_2$ ,  $\text{TiO}_2$ ,  $\text{Cr}_2\text{O}_3$ ,  $\text{Fe}_2\text{O}_3$ ,  $\text{P}_2\text{O}_5$  were then commonly added to the parent silicate glass composition to initiate the nucleation process [10,11,54,59,61-63].

$\text{Cr}_2\text{O}_3$  can remarkably increase the crystallization rate mostly for Fe-containing glass compositions as the corresponding mechanism includes the formation of spinel which, in turn, actively catalyses the formation of pyroxene phases [65-73]. Karamanov et al. [65] demonstrated that the  $\text{Cr}_2\text{O}_3$  addition, in percentages as high as 0.7

wt.%, enhances the spinel formation which, accordingly, increases the number of nuclei available for crystallisation; as a result, a higher degree of crystallisation and a finer structure of the glass-ceramic was achieved. The effect of  $\text{Cr}_2\text{O}_3$  on glass crystallization can be studied by comparing the position of the exothermic peaks in the DTA thermograms for different compositions (Fig. 5): as the  $\text{Cr}_2\text{O}_3$  content increases, there is a sharpening effect on the shape of the peak along with the shift of  $T_c$  and  $T_p$  towards lower values.

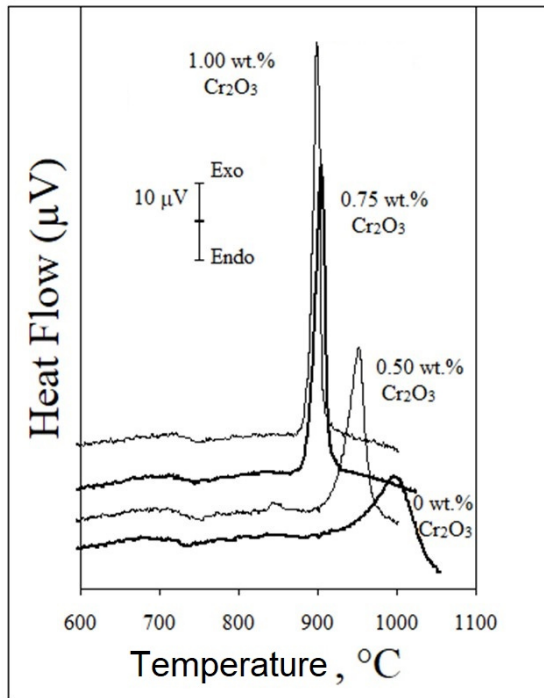


**Fig. 5.** DTA plots of glass powders with different  $\text{Cr}_2\text{O}_3$  content [72,73].

The crystallization of a major phase may be initiated by a liquid-liquid phase separation without the need for a crystalline nucleation catalyst. Such separation may result in a fine-scale dispersion of second-phase liquid droplets that are very poor glass formers and, therefore, crystallize very readily [63]. In turn, the addition of some nucleation agents such as  $\text{ZrO}_2$ ,  $\text{TiO}_2$ ,  $\text{P}_2\text{O}_5$ ,  $\text{Ta}_2\text{O}_5$ ,  $\text{WO}_3$ ,  $\text{Fe}_2\text{O}_3$  and F was reported to cause the formation of primary crystals in the systems  $\text{Li}_2\text{O}-\text{Al}_2\text{O}_3-\text{SiO}_2$  and  $\text{MgO}-\text{Al}_2\text{O}_3-\text{SiO}_2$ ; these nucleation agents were also shown to accumulate in a specific microphase of phase-separated base glass or, in general, to promote phase separation. Höland and Beall [10] pointed out that “for most commercially significant glass-ceramics, heterogeneous nucleation of the base glass has been achieved with targeted development and utilization of microimmiscibility”. For instance,  $\text{P}_2\text{O}_5$  as nucleating agent caused microphase separation inducing the formation of the transition phase  $\text{Li}_3\text{PO}_4$  prior to the crystallization of lithium disilicate [10]. Likewise, it is worth men-

tioning that, in tetrasilicic mica glasses, Mg-, K- and F-rich droplets can precipitate in a silicate matrix phase [74,75]. Furthermore, as regards the behaviour of glasses from tetrasilicic mica ( $\text{KMg}_{2.5}\text{Si}_4\text{O}_{10}\text{F}_2$ )–fluorapatite ( $\text{Ca}_5(\text{PO}_4)_3\text{F}$ )–diopside ( $\text{CaMgSi}_2\text{O}_6$ ) system (Fig. 6), it was revealed that mica crystallites were formed from fine-scaled glass-in-glass phase separation containing quasi-spherical mica grains [75]. In this regard, Fig. 7,a shows the microstructure of glass corresponding to tetrasilicic mica composition in which round-shaped particles (diameter 0.6-1.0  $\mu\text{m}$ ) were embedded in glassy matrix. Interestingly, the nucleation of apatite and diopside might be obtained simultaneously to the formation of tetrasilicic mica in the tetrasilicic mica–fluorapatite–diopside system. It is likely that nucleation is achieved within the droplet glass phases, and phase separation is further enhanced with the addition of CaO and  $\text{P}_2\text{O}_5$  introduced through apatite and diopside. The tendency of glasses to favour phase separation as well as the formation of large spherical droplets yield important optical effects, such as high opacity (light scattering) resulting in the milky appearance of glasses containing apatite and diopside (Fig. 8). The glass compositions mentioned above are preferably crystallized in bulk form within 700-1075  $^\circ\text{C}$  [75]. Looking at the diagram in Fig. 6, tetrasilicic mica is crystallized from glass 1: for example, a typical “house of card” structure of randomly-oriented block-like mica crystals (1.5–3.0  $\mu\text{m}$ ) is formed when the base glass 1 is thermally treated at 1075  $^\circ\text{C}$  for 5 h (Fig. 7,b). The other intermediate glasses 2, 3 and 4 (see Fig. 6) can crystallize yielding a combination among mica, apatite and diopside.

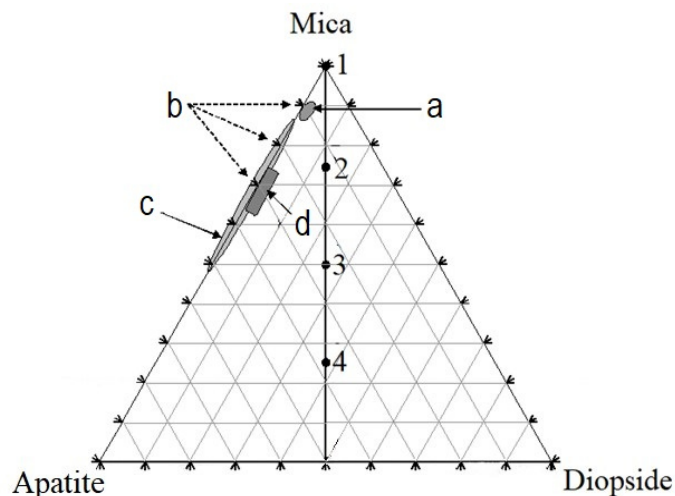


**Fig. 6.** Position of four different glasses in the tetrasilicic mica (M) -fluorapatite (FA) –diopside (D) system. **1:** glass of tetrasilicic mica composition (M) , **2:** 75.0% M, 12.5% FA, 12.5% D, **3:** 50.0% M, 25.0% FA, 25.0% D, **4:** 25.0% M, 37.5% FA, 37.5% D. For comparison, some compositions that have been already reported in the references 76, 77, 78 and 79 are labelled in the diagram as a, b, c and d, respectively.

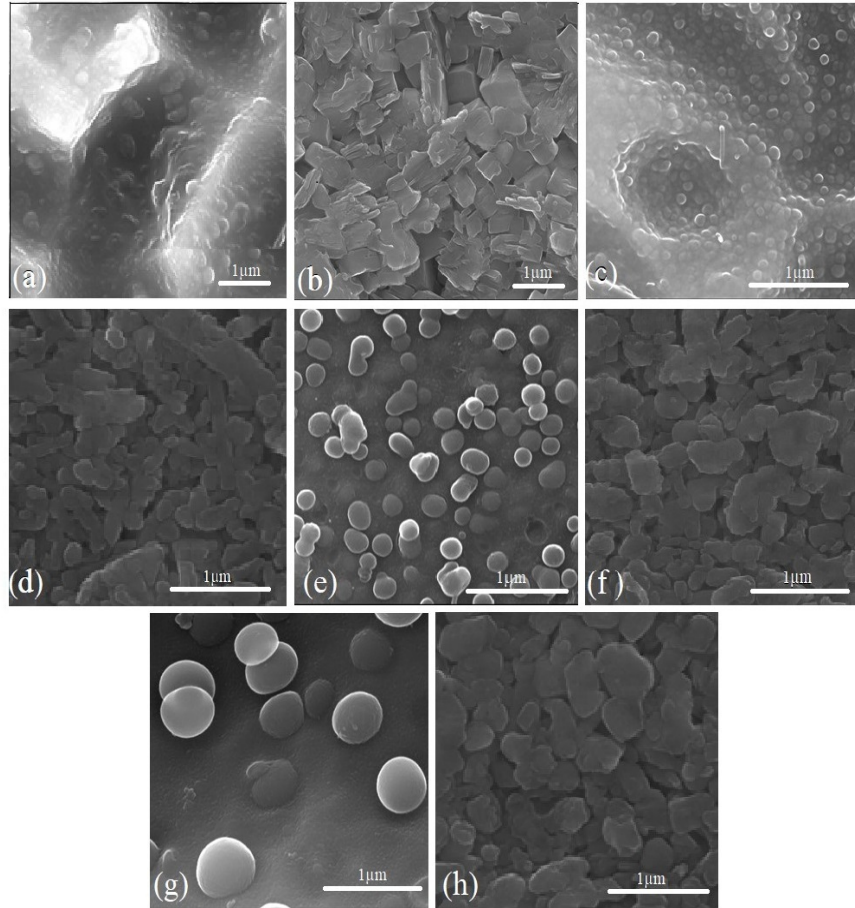


**Fig. 7.** Microstructure of annealed glasses (position of the compositions are shown in the ternary diagram of Fig. 6) (a) 1, (c) 2, (e) 3, (g) 4, and corresponding glass-ceramics (b) 1 (1075°C, 5 h), (d) 2 (1000°C, 1 h), (f) 3 (1000°C, 2 h), (h) 4 (1050°C, 1 h) in tetrasilicic mica ( $\text{KMg}_{2.5}\text{Si}_4\text{O}_{10}\text{F}_2$ )–fluorapatite ( $\text{Ca}_5(\text{PO}_4)_3\text{F}$ )–diopside ( $\text{CaMgSi}_2\text{O}_6$ ) system [75].



**Fig. 8.** From the right to the left: pattern of the annealed glass 2 (rightmost), annealed glass 3 (in the center of the figure) and pattern of the glass 3 heat treated at 1000°C for 2 h (see also Fig. 6).

## 7 Monitoring the crystallization in glass-ceramics

Glass-ceramics are fine-grained polycrystalline materials formed when glasses of suitable compositions are heat-treated and undergo controlled crystallization (devitrification). While glasses, in principle, can be prepared from a variety of substances including inorganic materials, organics, metals and even polymers, the term glass-ceramics is typically used for inorganic, non-metallic materials [80].

The key feature of the processing of glass-ceramics is that the crystallization must be controlled. One or more crystalline phases may form during the heat treatment, and both the composition of these phases and the composition of the residual glass are normally different from that of the parent glass [5,10,11,54,61, 81,82]. The content of crystalline phase(s) may vary between 0.5 and 99.5%, but in most applications the crystalline volume fraction is in the range of 30 to 70% [59]. The broader range was achieved by Deubener et al. [80], who reported volume fractions of crystalline phase in the range of few ppm to almost 100%.

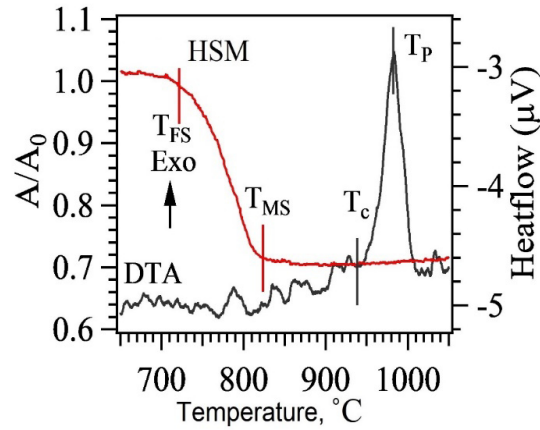
Glass-ceramics are highly appealing for several end applications, such as the thermal, chemical, biological and dielectric ones, because the properties of these materials (e.g. transparency, mechanical strength, resistance to abrasion, coefficient of thermal expansion etc.) can be finely modulated by properly selecting the parent glass composition and the heat-treatment parameters (temperature, time, oxidizing vs. reductant atmosphere), which can control the extent of crystallization, crystal morphology, crystal size and aspect ratio.

The ease of fabrication techniques and relatively low production cost offer obvious industrial advantages [5,10,11,54,61, 82]. Initially, the glass batch is heated to form a

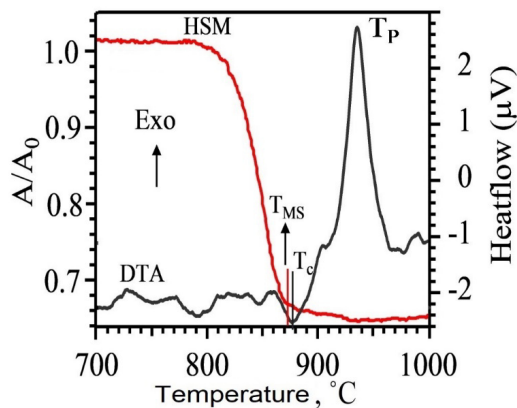
homogeneous melt. Then, the desired shape of the product is obtained by applying processes such as pressing, blowing, rolling or casting to the glass at the working point, which corresponds to a viscosity of about  $10^3$  Pa·s. After being annealed to eliminate internal stresses, the glass product finally undergoes a thermal treatment that converts it into a glass-ceramic [83]. The properties of these materials, especially the mechanical ones (e.g. bending strength, hardness, toughness), are superior to those of most conventional glass and even traditional ceramic materials.

Glass-ceramics are often produced according to controlled nucleation and crystal growth in the volume of the parent glass. However, if the specific surface area of the system is high, crystallization can start from the surface: this is the typical case of glass-ceramics produced by concurrent sinter-crystallization of glass powder compacts (greens). In this case, nucleating agents are not required because the particle surfaces provide nucleation sites and crystallization starts at the interfaces among glass particles [59]. DTA thermographs combined with HSM may serve as useful, complementary instruments for monitoring – and then optimizing – the sintering and crystallization processes. In particular, the glass stability against crystallization can be measured by using the thermal parameters already defined in the section 2 (e.g.  $K_H$  and  $S_c$ ). In general, glasses with a large temperature interval between onset of crystallization and  $T_g$  (also called “sintering window”) can possibly be well sintered [84]. When the onset of crystallization occurs before the glass is fully densified, further densification will be impeded by the formation of crystalline phase(s) that increase(s) the matrix viscosity [85].

HSM allows the sintering processes to be studied in a “real-time” mode, since it permits glass scientists to follow continuously the contraction process without any external load or friction. Small greens with cylindrical geometry are commonly used in HSM-based sintering studies, so that the axial and radial contractions of the powder compact can be simultaneously recorded, and the anisotropy during sintering can be determined. The HSM projects the silhouette of the sample through a quartz window and onto the recording device; an image analysis system automatically records and analyses the geometrical changes of the sample (e.g. shrinkage or blowing) during heating. The image analyser takes into account the thermal expansion of the alumina substrate while measuring the height of the sample during controlled heating, with the base as a spatial reference. Complementary studies using DTA and HSM under the same heating conditions are therefore very useful for investigating the effect of glass composition on sintering and devitrification phenomena. In general, the desired order of events in glass-powder densification processes occurs when sintering precedes crystallization. This is key to obtain a final high-density material with very low porosity like, for instance, a gas-tight glass–ceramic seal [86] (Fig. 9). On the contrary, if crystallization occurs before sintering is completed (Fig. 10), the viscosity increases sharply and sintering is highly inhibited or even stops.

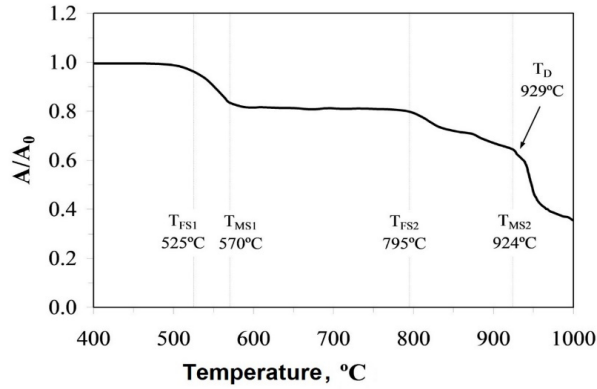


**Fig. 9.** An example illustrating the relationships between the HSM and DTA data for diopside glass system [87] ( $T_{FS}$ : first shrinkage,  $T_{MS}$ : maximum shrinkage,  $T_c$ : onset of crystallization, and  $T_p$ : peak crystallization temperature).



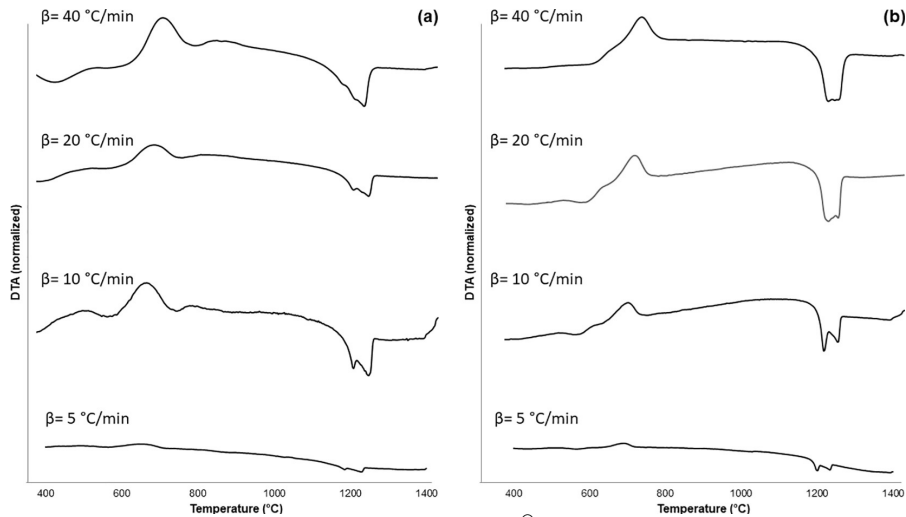
**Fig. 10.** An example illustrating the relationships between the HSM and DTA data for melilite glass [88] system ( $T_{FS}$ : first shrinkage,  $T_{MS}$ : maximum shrinkage,  $T_c$ : onset of crystallization, and  $T_p$ : peak crystallization temperature).

Fig. 11 displays another interesting scenario in which glass powder sintering was partially impeded by crystallization. HSM investigation on glass powder compact revealed the presence of two densification steps (i.e.  $T_{FS1} - T_{MS1}$  and  $T_{FS2} - T_{MS2}$ ) that are separated by the temperature range in which crystallization occurs and temporarily stops sintering. At the end of the second densification step, a total variation of  $A/A_0$  close to 0.60 was achieved, corresponding to volume shrinkage of about 40% (under the hypothesis of isotropic shrinkage) and to a practically full densification of the sample.



**Fig. 11.** Variation in relative area of powder sample's silhouette ( $A/A_0$ :  $A_0$  is the initial area at room temperature,  $A$  is the area at defined temperature) during the HSM measurement.

It was also demonstrated that the glass particle size and the heating rate have an effect on crystallization. Specifically, the finer the particles for a given glass composition, the lower  $T_g$  and  $T_p$ , provided that all the other experimental conditions are kept constant [89,90]. This means that a glass powder compact composed by small particles will undergo concurrent crystallization during sintering at lower temperatures as compared to a similar sample of coarser particles. In the same studies,  $T_g$  and  $T_p$  were also observed to increase as the heating rate increased (Fig. 12).



**Figure 12.** DTA thermographs of Bioglass® powders (composition 45SiO<sub>2</sub>-24.5CaO-24.5Na<sub>2</sub>O-6P<sub>2</sub>O<sub>5</sub> wt.%) having different size – (a) less than 5 μm and (b) less than 32 μm – and collected at different heating rates ( $\beta$ ).

DTA or DSC also are quite popular methods for studying the kinetics of crystallization processes in glasses. The crystallization kinetics based on these data are usually interpreted according to the Avrami nucleation-growth model and the Johnson-Mehl-Avrami equation [91], which describes the time (t) dependence of the crystallized fraction  $\alpha$  as follows:

$$(-\ln(1 - \alpha))^{1/n} = kt \quad (3)$$

where k and n (Avrami coefficient) are constant.

The value of n can be related to another parameter, called m, which is the dimensionality of growth of the crystalline phase [92]. The values of m range from 1 (1-dimensional growth corresponding to rod-like crystals) to 3 (3-dimensional growth corresponding to sphere-like crystals); if surface crystallization is dominant, there is the condition  $n = m = 1$ . Kinetic aspects of crystallization in glasses and amorphous solids have been comprehensively reviewed and discussed by Malek [93,94].

## 8 Glass-ceramic types and applications

Over many years, silicate systems were extensively used for developing glass-ceramics for commercialization purposes. Although many other systems are now subject of intense research [80], silicate systems will be inevitably elaborated yet more considering their high flexibility in compositional design and versatility for myriads of applications, ease of processing due to their appropriate glass forming ability, abundance of precursors in the Earth crust, etc. The design of glass-ceramic products takes into account multiple factors, including requirements for external contours, color and aesthetics, surface structure and internal microstructure in relation to the functional properties [10]. The microstructure of glass-ceramics coupled with the phase assemblage (i.e. type of crystalline phase(s), volume fraction of crystalline and glassy constituents) dictate the final functional properties of the product (e.g. resistance to wear, toughness etc.) while the parent glass composition is key to determine the degree of glass workability and to foresee whether internal or surface nucleation can be achieved [10]. Too high rates of crystal growth are to be avoided; materials in which the crystal growth rate is too high do not develop the fine-grained microstructure, necessary for the achievement of high mechanical strength. The major components of any glass-ceramic composition are selected to ensure precipitation of crystalline phase(s) that will impart desired properties but also bearing in mind the need for producing a glass melt with proper viscosity-temperature characteristics to be shaped by using the available techniques.

Just to cite a few examples, the beta-quartz and kyanite solid solutions, spodumene or beta-eucryptite are predominantly precipitated in glass-ceramics under tightly controlled conditions in order to achieve zero thermal expansion and make useful materials for transparent cookware, optics, telescope mirror blanks, infrared transmitting electric range tops, wood-stove windows and fire door glazing where the dimensional stability and the ability to resist thermal shock are necessary [95,96]. High-strength glass-ceramics may contain spinel, mullite and corundum, while glass-ceramics for electrical applications include cordierite, anorthite, diopside and wollastonite [54,61].

Commercial glass-ceramics can be divided in several categories according to their applications, which may be addressed to both high-tech and more common uses, including glass-ceramics for thermal protection, machinable glass-ceramics, high-strength glass-ceramics, glass-ceramics for biomedical applications, glass-ceramics for electrical and electronic applications, optical glass-ceramics, glass-ceramics used as construction materials., etc. [10,54,59,61]. Commercial glass-ceramics for broad consumer and specialized markets are currently produced by several companies all around the world such as Corning, Schott AG, St. Gobain, Nippon Electric Glass, Ohara, Ivoclar etc. One of the most comprehensive analyses of glass-ceramic commercialization was provided by Maziar et al. in 2015 [97], who performed a detailed patent search and reported that glass-ceramics with specific properties, such as thermal (e.g., low thermal expansion, insulating, high thermal stability, etc.), electrical, (e.g., high ionic conductivity), or optical (e.g., high transparency, high luminescence efficiency) ones, have mainly attracted the attention from companies over the past decade. The range of applications was quite broad (Fig. 13), spanning from more “traditional” fields, such as chemistry, engineering, energy, materials science and medicine, to unusual areas, such as polymer science and food technology (also food packaging). More specifically, above 550 patents on various glass-ceramics for making electronic components, wiring board substrates, cooktop panels, insulators, sealants and heat reflector substrates were found. Some other patents have been granted for glass-ceramics addressed to architectural, biomedical, magnetic, armor, energy, nuclear, and waste immobilization applications. Overall, two opposite trends were found in patent applications for glass-ceramics, i.e. (i) a decrease of electrical, electronic and magnetic applications and (ii) an increment of dental, biomedical, optical, energy, chemical, waste management and refractory. These trends are actually in line with current demands of new high-tech products, thus suggesting prospects for industrial growth of glass-ceramic market in these areas.

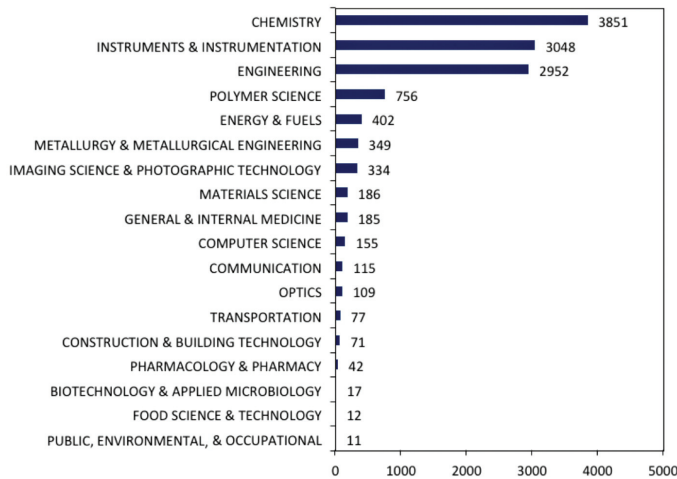


**Figure 13.** Breakdown from the Derwent World Patent Index (DWPI) database about the number of patents granted in various fields from 1968 to 2014 by using the keywords “glass-ceramic\*” or “glass ceramic\*”.

## 9 A forecast for the future: the potential of modelling and computational approaches in the “glass and glass-ceramic world”

Although being an ancient, traditional material, glass – along with its glass-ceramic derivatives – does not stop yet proving to be suitable in a number of new, high-tech fields. Many of these latest applications are described in the next chapters of this book, including the uses of glass and glass-ceramics in medicine, optics and optoelectronics, energy storage and circular economy.

The relatively recent success of many glass-ceramic products relies on achieving unique combinations of attributes, including appropriate optical, thermal, mechanical, and biological properties, which often cannot be achieved by using an amorphous glass. Machinability is another key technological added value of many glass-ceramics for such applications.

Even though the thermodynamic and kinetic aspects of sintering and crystallization are crucial for designing industrial materials, the theoretical understanding of these basic processes still is incomplete. Future development of new rigorous or even computational models will hopefully enable more accurate quantitative predictions of glass and glass-ceramic properties

As a general comment, we think that the progress of glass/glass-ceramic science and technology in these so advanced fields will benefit from an ever stronger combination between theoretical aspects and computational approaches. Mathematical and numerical modelling is very helpful not only to shed light on the basic aspects of glass structure, but also to better describe and, to some extent, predict the functional properties of glasses. Conventional empirical, trial-and-error approaches for developing new glasses and characterizing their properties are expensive and time-consuming. In order to overcome these limitations, modelling has been emerging as a significant component of research in glass science and technology. Just to mention a famous and well-known example, the software SciGlass is able to implement a series of empirical and semi-empirical models based on large datasets to estimate the main physical, thermal and mechanical properties of a variety of glasses after receiving the oxide composition (wt.% or mol.%) as the input. These predictions are very useful to perform a preliminary selection of glass candidates for a given application and refine the composition in the attempt to achieve the desired target properties [98].

At present, a variety of computational techniques are available to researchers, such as those based on machine learning or molecular dynamics. A number of models are available as well, from purely empirical models relying on the mathematical interpolation of experimental data to ab-initio methods needing a detailed description of the material’s electronic structure [99].

While many of these modelling approaches are potentially applicable to any class of materials, some methods (e.g. the topological constraint theory that describes the connectivity of disordered glassy networks) have been specifically developed for modelling amorphous or partially-amorphous systems such as glasses and glass-ceramics. The appropriate choice of modelling technique depends on the nature of the system under investigation, the desired properties to estimate, the quality and availability of existing data, and the level of physical understanding behind the structure-

property relationships in that system. A combination of multiple modelling approaches can often be beneficial. Indeed, all models need to be validated by experiments; therefore, cross-disciplinary collaboration among glass researchers, mathematicians and data/computer scientists will be more than ever necessary.

## References

1. Doremus, R.H.: *Glass Science*. Wiley, New York (1994).
2. Gutzow, I., Schmelzer, J.: *The vitreous state*. Springer-Verlag, Berlin (1995).
3. Paul, A.: *Chemistry of Glasses*. 2nd ed. Chapman and Hall, London (1990).
4. Rawson, H.: *Inorganic Glass Forming Systems*. Pergamon Press, New York (1967).
5. Shelby, J.E.: *Introduction to glass science and technology*. The Royal Society of Chemistry, Cambridge (1997).
6. Varshneya, A.K.: *Fundamentals of Inorganic Glasses*. Academic Press, London (1994).
7. Vogel, W.: *Structure and crystallization of glass*. Pergamon press, Lipzig (1971).
8. Zarzycki, J.: *Glasses and the Vitreous State*. Cambridge University, Cambridge (1991).
9. Phillips, C.J.: *Glass, the miracle maker: its history, technology, manufacture and applications*. 2nd ed. Pitman, New York (1948).
10. Höland, W., Beall, G.: *Glass-ceramic Technology*. The American Ceramic Society, Westerville, Ohio (2002).
11. McMillan, P.W.: *Glass-Ceramics*. Academic Press, London (1979).
12. Le Bourhis, E.: *Glass: Mechanics and Technology*. Wiley-VCH Verlag, Weinheim (2008).
13. Scholze, H.: *Glass: Nature, Structure and Properties*. Springer, Berlin (1991).
14. Harper, C.A.: *Handbook of Ceramics, Glasses and Diamonds*. McGraw-Hill, New York (2001).
15. C162 -Compilation of ASTM Standard Definitions. Philadelphia: The American Society for Testing Materials (1945).
16. Varshneya, A.K., Mauro, J.C.: Comment on misconceived ASTM definition of glass by A. C. Wright. *Glass Technology: European Journal of Glass Science and Technology Part A* 51(1), 28-30 (2010).
17. Zanutto, E.D., Mauro J.C.: The glassy state of matter: Its definition and ultimate fate. *J Non-Cryst Solids* 471, 490–495 (2017).
18. Schmelzer, J.W.P., Tropin, T.V.: Glass Transition, Crystallization of Glass-Forming Melts, and Entropy. *Entropy* 20,103 (2018).
19. Ojovan, M.I.: Ordering and structural changes at the glass-liquid transition. *J Non-Cryst Solids* 382, 79-86 (2013).
20. Goldschmidt, V.M.: *Geochemische Verteilungsgesetze der Elemente*. Skrifter Norske Videnskaps-Akademie, Oslo (1926).
21. Zachariasen, W.H.: The atomic arrangement in glass. *J Am Chem Soc* 54(10), 3841-3851 (1932).
22. Warren, B.E.: X-ray determination of the structure of glass. *J Am Ceram Soc* 17(1-12), 249–254 (1934).
23. Wright, A.C. Neutron and X-ray amorphography. *J Non-Cryst Solids* 106(1-3), 1-16 (1988).
24. Jiang, Z.-H., Zhang, Q.-Y.: The structure of glass: A phase equilibrium diagram approach. *Prog Mater Sci* 61, 144-215 (2014).

25. Cabral, A.A., Cardoso, A.A.D., Zanotto, E.D.: Glass-forming ability versus stability of silicate glasses. I. Experimental. *J Non-Cryst Solids* 320, 1-8 (2003).
26. Hrubý, A.: Evaluation of Glass-Forming Tendency by Means of DTA, *Czech J Phys* 22, 1187-1193 (1972).
27. Turnbull, D., Cohen, M.: *Crystallization Kinetics and Glass Formation*. Butterworths, London (1960).
28. Avramov, I., Zanotto, E.D., Prado, M.O.: Glass-forming ability versus stability of silicate glasses. II. Theoretical demonstration. *J Non-Cryst Solids* 320, 9-20 (2003).
29. Uhlmann, D.R.: A kinetic treatment of glass formation. *J Non-Cryst Solids* 7(4), 337-348 (1972).
30. Weinberg, M.C., Uhlmann, D.R., Zanotto, E.D.: 'Nose method' of calculating critical cooling rates for glass formation. *J Am Ceram Soc* 72, 2054-2058 (1989).
31. Weinberg, M.C., Zanotto, E.D.: Calculation of the volume fraction crystallised in nonisothermal transformations. *Phys Chem Glasses* 30(3), 110-115 (1989).
32. Uhlmann, D.R., Zelinski, B.J.J., Zanotto, E.D., Weinberg, M.C.: Sensitivity of critical cooling rate to model and material parameters. Paper presented at: XV International Congress on Glass, Leningrad, USSR (1989).
33. Weinberg, M.C.: Glass-forming ability and glass stability in simple systems. *J Non-Cryst Solids* 167(1-2), 81-88 (1994).
34. Cabral Jr., A.A., Fredericci, C., Zanotto, E.D.: A test of the Hrubý parameter to estimate glass-forming ability. *J Non-Cryst Solids* 219, 182-186 (1997).
35. Panda, P.C., Raj, R.: Sintering and Crystallization of Glass at Constant Heating Rate, *J Am Ceram Soc* 69, 1564-1566 (1989).
36. Ferraris, M., Verné, E.: Viscous Phase Sintering of Particle-Reinforced Glass Matrix Composites. *J Eur Ceram Soc* 16, 421-427 (1996).
37. Lara, C., Pascual, M.J. Duran, A.: Glass-Forming Ability, Sinterability and Thermal Properties in The System RO-BaO-SiO<sub>2</sub> (R = Mg, Zn). *J Non-Cryst Solids* 348, 149-155 (2004).
38. Baine, F., Ferraris, M., Bretcanu, O., Verné, E., Vitale-Brovarone, C. Optimization of composition, structure and mechanical strength of bioactive 3-D glass-ceramic scaffolds for bone substitution. *J Biomater Appl* 27, 872-890 (2013).
39. Hench, L.L., West, J.K.: The sol-gel process. *Chem Rev* 90, 33-72 (1990)
40. Baine, F., Fiume, E., Miola, M., Verné, E.: Bioactive sol-gel glasses: Processing, properties, and applications. *Int J Appl Ceram Technol* 15, 841-860 (2018).
41. Rao, K.J.: *Structural chemistry of glasses*. Elsevier Science & Technology Books, Amsterdam (2002).
42. Jones, G.O.: *Glass*. Wiley, Methuen (1956).
43. Kurkjian, C.R., Prindle, W.R.: Perspectives on the History of Glass Composition. *J Am Ceram Soc* 81(4), 795-813 (1998).
44. Yamane, M., Asahara, Y.: *Glasses for photonics*. Cambridge University Press, Cambridge (2004).
45. Wright, A.C., Bachra, B., Brunier, T.M., Sinclair, R.N., Gladden, L.F., Portsmouth, R.L.: A neutron diffraction and MAS-NMR study of the structure of fast neutron irradiated vitreous silica. *J Non-Cryst Solids* 150(1-3), 69-75 (1992).
46. Kirk, R.E., Othmer, D.F., Grayson, M., Eckroth, D.: *Encyclopedia of chemical technology*. 5th ed. John Wiley & Sons, New Jersey (2007).
47. Bergeron, C.G., Risbud, S.H.: *Introduction to Phase equilibria in Ceramics*. The American Ceramic Society, Westerville, Ohio (1984).

48. Morey, G.W., Bowen, N.L.: Ternary System Sodium Metasilicate-Calcium Metasilicate-Silica. *J Glass Technol Soc* 9(35), 226-264 (1925).
49. Morey, G.W.: The Devitrification of Soda-Lime-Silica Glasses. *J Am Ceram Soc* 13, 683-713 (1930).
50. Segnit, E.R., Further Data on the System  $\text{Na}_2\text{O-CaO-SiO}_2$ . *Am J Sci* 251(8), 586-601 (1953).
51. Toropov, N.A. et al.: Phase Diagrams of Silicate Systems: Handbook; third Issue; Ternary Systems, Nauka, Leningrad (1972); Translation, Army Foreign Science and Technology Center Charlottesville, Virginia, 10 June 1974.
52. Artamonova, M.V., Aslanova, M.S., Buzhinsky, I.M.: Chemical technology of glasses and glass-ceramics, Edited by Pavlushkin N.M., Stroiizdat, Moscow (1983).
53. Baino, F., Quaglia, A.: Evidences of glass-ceramic white opaque tesserae from Roman age: A thermo-analytical approach. *Mater Lett* 74, 194-196 (2012).
54. Pavlushkin, N.M.: Principles of glass-ceramic technology. Stroiizdat, Moscow (1979) (in Russian).
55. Réaumur, R.A.M.: Art de faire une nouvelle espèce de porcelaine, par des moyens extrêmement simples et faciles, ou de transformer le Verre en Porcelaine (Art of a new porcelain species, extremely simple and easy ways, or how to transform Glass into Porcelain). *Hist Acad R Sci Paris* 1, 370-388 (1739).
56. Woodard, K.L.: Profiles in ceramics. S. Donald Stookey. *Am Ceram Soc Bull* 3, 34-39 (2000).
57. Stookey, S.D.: Chemical machining of photosensitive glass. *Ind Eng Chem* 45(1), 115-118 (1953).
58. Stookey, S.D.: Catalyzed Crystallization of glass in theory and practice. *Ind Eng Chem* 51(7), 805-808 (1959).
59. Zanotto, E.D.: A bright future for glass-ceramics. *Am Ceram Soc Bull* 89(8), 19-27 (2010).
60. Tammann, G.: Glasses as super-cooled liquids. *J Soc Glass Technol* 9, 166-185 (1925).
61. Strnad, Z.: Glass-ceramic materials. Elsevier, Amsterdam (1986).
62. Lewis, M.H., Metcalf-Johansen, J., Bell, P.S.: Crystallization mechanism in glass-ceramics. 62(5-6), 278-288 (1978).
63. Pinkney, L.R.: Glass ceramics. In: Buschow, K.H.J., Cahn, R., Flemings, M.C., Ilshner, B., Kramer, E.J., Mahajan, S., et al. (Eds.), *Encyclopedia of Materials: Science and Technology*, Pergamon, Oxford (2001).
64. Borrelli, N.F.: Photosensitive glass and glass ceramics. CRC Press, Taylor & Francis Group, Corning Inc., Corning, New York, USA (2017).
65. Karamanov, A., Piscicella, P., Pelino, M.: The Effect of  $\text{Cr}_2\text{O}_3$  as a Nucleating Agent in Iron-rich Glass-ceramics. *J Eur Ceram Soc* 19, 2641-2645 (1999).
66. Besborodov, M.A.: Glass-Ceramic Materials. Nauka i Technika, Minsk (1982) (in Russian).
67. Rawlings, R.D.: Production and properties of silceram glass-ceramics. In: *Glass-Ceramic Materials, Fundamentals and Applications Series of Monographs on Material Science, Engineering and Technology*. Mucchi Editore, Modena, 115-133 (1997).
68. Zhunina, L., Kuzmenkov, M., Yaglov, V.: Pyroxene Sitalls. University Publishers, Minsk (1974) (in Russian).
69. Alizadeh, P., Marghussian, V.K. : The effect of compositional changes on the crystallization behavior mechanical properties of diopside-wollastonite glass-ceramics in the  $\text{SiO}_2\text{-CaO-MgO-Na}_2\text{O}$  system. *J Eur Ceram Soc* 20, 765-773 (2000).

70. Rezvani, M., Eftekhari-Yekta, B., Solati-Hashjin, M., Marghussian, V.K.: Effect of  $\text{Cr}_2\text{O}_3$ ,  $\text{Fe}_2\text{O}_3$  and  $\text{TiO}_2$  nucleants on the crystallization behaviour of  $\text{SiO}_2\text{-Al}_2\text{O}_3\text{-CaO-MgO}$  ( $\text{R}_2\text{O}$ ) glass-ceramics. *Ceram Int* 31, 75-80 (2005).
71. Karamanov, A., Arrizza, L., Matekovits, I., Pelino, M.: Properties of sintered glass-ceramics in the diopside–albite system. *Ceram Int* 30, 2129–2135 (2004).
72. Vasilopoulos, K.C., Tulyaganov, D.U., Agathopoulos, S., Karakassides, M.A., Ferreira, J.M.F., Tsipas, D.: Bulk nucleated fine grained mono-mineral glass-ceramics from low-silica fly-ash. *Ceram Int* 35(2), 555-558 (2009).
73. Vasilopoulos, K.C., Tulyaganov, D.U., Agathopoulos, S., Ribeiro, Karakassides, M.A., Ferreira, J.M.F., Tsipas, D.: Vitrification of low-silica fly-ash. Suitability of the resulting glass-ceramics for architectural or electrical insulator applications. *Adv Appl Ceram* 108(1), 27-32 (2009).
74. Vogel, W.: *Chemistry of Glass*. The American Ceramic Society, Westerville, Ohio (1985).
75. Tulyaganov, D.U., Agathopoulos, S., Fernandes, H.R., Ventura, J.M., Ferreira, J.M.F.: Crystallization of glasses in the system tetrasilicic mica-fluorapatite-diopside. *J Eur Ceram Soc* 24(13), 3521-3528 (2004).
76. Hamzawy, E.M.A.: Crystallization behaviour of fluorphlogopite glass-ceramics. *Ceram Silikaty* 45, 89-96 (2001).
77. Taruta, S., Mukoyama, K., Suzuki, S.S., Kitajima, K., Takusagawa, N.: Crystallization process and some properties of calcium mica-apatite glass-ceramics. *J Non-Cryst. Solids* 296, 201-211 (2001).
78. Höland, W., Vogel, W.: Machinable and phosphate glass-ceramics. In: *An Introduction to Bioceramics*. Hench, L.L., Wilson J. (Eds.), World Scientific, Singapore, 125-137 (1993).
79. Chen, X., Hench, L., Greenspan, D., Zhong, J., Zhang, X.: Investigation on phase separation, nucleation and crystallization in bioactive glass-ceramics containing fluorphlogopite and fluorapatite. *Ceram Int* 24, 401-410 (1998).
80. Deubener, J. et al.: Updated definition of glass-ceramics. *J Non-Cryst Solids* 501, 3-10 (2018).
81. James, P.F.: *Glasses and Glass-Ceramics*. Chapman and Hall, London (1989).
82. Rawlings R.D., Wu, J.P., Boccaccini A.R. Glass-ceramics: Their production from wastes—A Review. *J Mater Sci* 41, 733-761 (2006).
83. Carter, C.B., Norton, M.G.: *Ceramic materials - Science and engineering*. Springer, New York (2007).
84. Siligardi, C., D'Arrigo, M.C., Leonelli, C.: Sintering behavior of glass-ceramic frits. *Am Ceram Soc Bull* 79(9), 88-92 (2000).
85. Boccaccini, A.R., Stumpfe, W., Taplin, D.M.R., Ponton, C.B.: Densification and crystallization of glass powder compacts during constant heating rate. *Mater Sci Eng A* 219, 26-31 (1996).
86. Tulyaganov, D. U., Reddy, A., Kharton, V.V., Ferreira, J.M.F.: Aluminosilicate-based sealants for SOFCs and other electrochemical applications—A brief review. *J Power Sources* 242(15), 486-502 (2013).
87. Reddy, A.A., Tulyaganov, D.U., Pascual, M.J., Kharton, V.V., Tsipas, E.V., Kolotygin, V.A., Ferreira, J.M.F.: Diopside–Ba disilicate glass–ceramic sealants for SOFCs: stabilizing thermal parameters and improving adhesion to interconnects by Sr for Ca substitution. *Int J Hydrogen Energy* 38, 3073-3086 (2013).
88. Reddy, A.A., Tulyaganov, D.U., Kapoor, S., Goel, A., Pascual, M.J., Kharton, V.V., Ferreira, J.M.F.: Study of melilite based glasses and glass–ceramics nucleated by  $\text{Bi}_2\text{O}_3$  for functional application. *RSC Adv* 2, 10955-10967 (2012).

89. Sabato, A.G., Salvo, M., De Miranda, A., Smeacetto, F.: Crystallization behaviour of glass-ceramic sealant for solid oxide fuel cells. *Mater Lett* 141, 284–287 (2015).
90. Baino, F., Fiume, E.: Quantifying the effect of particle size on the crystallization of 45S5 bioactive glass. *Mater Lett* 224, 54–58 (2018).
91. Avrami, M.: Kinetics of phase change. I General theory. *J Chem Phys* 7, 1103–1112 (1939).
92. Matusita, K., Komatsu, T., Yokota, R.: Kinetics of non-isothermal crystallization process and activation energy for crystal growth in amorphous materials. *J Mater Sci* 19, 291–296, (1984).
93. Malek, J.: Kinetic analysis of crystallization processes in amorphous materials. *Thermochim Acta* 355, 239–253 (2000).
94. Malek, J.: Testing method for the Johnson–Mehl–Avrami equation in kinetic analysis of crystallization processes. *J Am Ceram Soc* 83, 2103–2105 (2000).
95. Krause, D., Bach, H. (Eds.): *Low Thermal Expansion Glass Ceramics*. Springer, Berlin (2005).
96. Vladislavova, L., Thieme, C., Zscheckel, T., Patzig, C., Rüssel, C.: Heterogeneous nucleation of  $\text{Ba}_{1-x}\text{Sr}_x\text{Zn}_2\text{Si}_2\text{O}_7$  from a BaO/SrO/ZnO/SiO<sub>2</sub> glass using platinum as nucleation agent. *J Eur Ceram Soc* 37, 4801–4808 (2017).
97. Montazerian, M., Prakash Singh, S., Zanotto, E.D.: An analysis of glass–ceramic research and commercialization. *Am Ceram Soc Bull* 94, 30–35 (2015).
98. Baino, F., Marshall, M., Kirk, N., Vitale-Brovarone, C.: Design, selection and characterization of novel glasses and glass-ceramics for use in prosthetic applications. *Ceram Int* 42, 1482–1491 (2016).
99. Montazerian, M., Zanotto, E.D., Mauro, J.C.: Model-driven design of bioactive glasses: from molecular dynamics through machine learning. *Int Mater Rev* 65, 297–321 (2020).